High Confinement and High Density with Stationary Plasma Energy and Strong Edge Radiation in the TEXTOR-94 Tokamak

A. M. Messiaen,[1,*] J. Ongena,[1,*] U. Samm,[2] B. Unterberg,[2] G. Van Wassenhove,[1] F. Durodie,[1] R. Jaspers,[3] M. Z. Tokaŕ,[2] P. E. Vandenplas,[1] G. Van Oost,[1] J. Winter,[2] G. H. Wolf,[2] G. Bertschinger,[2] G. Bonheure,[1] P. Dumortier,[1] H. Euringer,[2] K. H. Finken,[2] G. Fuchs,[2] B. Giesen,[2] R. Koch,[1] L. Könen,[2] C. Königs,[1] H. R. Koslowski,[2] A. Krämer-Flecken,[2] A. Lyssoivan,[1] G. Mank,[2] J. Rapp,[2] N. Schoon,[1] G. Telesca,[2] R. Uhlemann,[2] M. Vervier,[1] G. Waidmann,[2] and R. R. Weynants[1]

[1]*Laboratoire de Physique des Plasmas-Laboratorium voor Plasmafysica, Association "EURATOM-Belgian State," Ecole Royale Militaire, B 1000 Brussels, Koninklijke Militaire School, Belgium*

[2]*Institut für Plasmaphysik, Forschungszentrum Jülich, GmbH Association "Euratom-KFA," D-52425 Jülich, Federal Republic of Germany*

[3]*FOM Instituut voor Plasmafysica Rijnhuizen, Associatie "FOM-EURATOM," Nieuwegein, The Netherlands*

(Received 12 April 1996)

Stationary high energy confinement is observed on TEXTOR-94 for times limited only by the flux swing of the transformer using strong edge radiation cooling. Necessary tools are the feedback control of the radiated power and of the plasma energy content. At the highest densities obtained (up to 1.2 times the Greenwald limit), energy confinement exceeds the edge-localized-mode-free *H*-mode scaling ITERH93-P by more than 20%. β limits of TEXTOR-94 are reached with $f_{\mathrm{H89}}/q_a \approx 0.6$. No detrimental effect of the seeded impurity is seen. These high confinement discharges meet many conditions necessary for a fusion reactor regime. [S0031-9007(96)01240-9]

PACS numbers: 52.55.Fa

Several conditions have to be met simultaneously for an operational regime of a future fusion reactor. A sufficiently large energy confinement time should be realized to ignite the reactor plasma, and at the same time the problem of heat exhaust and ash removal must be solved for a steady state burn. The present reference scenario is the divertor *H* mode in order to obtain sufficient confinement. However, for a successful application of this regime to a fusion reactor, uncertainties still exist for the power threshold, the feasibility of the radiative divertor, its compatibility with edge localized modes (ELMs), and He exhaust.

It is therefore worthwhile to explore other regimes as well. It has been shown previously on TEXTOR that (i) improved confinement on a limiter machine is possible, without showing *H*-mode characteristics [1] as also observed on TFTR [2], (ii) a stable radiative edge with seeding of different impurities [3,4] can be established at a sufficiently high power flux to the wall without a shrinking of the plasma column [3,5] (so-called detachment), and (iii) transport is such that there is no harmful central impurity accumulation as a function of time [5]. In this paper we show that all these features can be combined in a positive way for long pulses at high plasma β and density by using feedback controls for the plasma β and for the radiated power P_{rad}. This regime could possibly serve as an alternative operational regime for a future fusion power reactor. Note that the compatibility of a radiating boundary in divertor configuration together with the observation of new confinement regimes has been recently reported by ASDEX-Upgrade [6].

TEXTOR-94 is a long-pulsed medium size circular limiter tokamak (major radius $R = 1.75$ m, minor radius $a = 0.46$ m, pulse lengths of about 10 s) equipped with the toroidal pumped belt limiter ALT-II [7]. The experiments described below are conducted at plasma currents between 280 and 480 kA and a toroidal magnetic field $B_t = 2.25$ T. Additional heating consists of coinjection ($D^+ \rightarrow D^0$ injection at about 50 keV) combined with ion cyclotron resonance heating (ICRH) at $\omega = 2\omega_{\mathrm{CD}}$ with π phasing of the two antenna pairs. In addition, the energy content of the discharges can be feedback controlled by applying a constant level of coinjection neutral beam power (NBI) and a variable level of ICRH. In this way, the effect of transport changes on β is compensated in real time by a changing amount of additional heating. The feedback control for the level of Ne VIII (which is roughly proportional to P_{rad}) is acting on the Ne inlet valve [3]. The presence of the pumped limiter is essential as a sink for Ne in the feedback loop and stationary plasmas are routinely obtained with a radiated power fraction $\gamma = P_{\mathrm{rad}}/P_{\mathrm{tot}}$ up to 90%, where P_{tot} is the total heating power applied. The radiation is monitored by a bolometric diagnostic allowing a 2D reconstruction of the radiation pattern in the discharge.

Characteristics of discharges in TEXTOR-94 with feedback controlled energy content and edge neon impurity seeding.—Figure 1(a) shows typical plasma parameters obtained in a Ne-cooled discharge where the total stored plasma energy is kept constant with a normalized toroidal $\beta_n \cong 1.65$ sufficiently below the limit $\beta_n \cong 2$ of the machine [1]. Omission of the energy feedback can lead to confinement transitions (with sometimes spectacular high β recoveries [8]) or disruptions. Remarkable in this figure is the value of the enhancement factor f_{H93} of the energy confinement time versus the recent reference

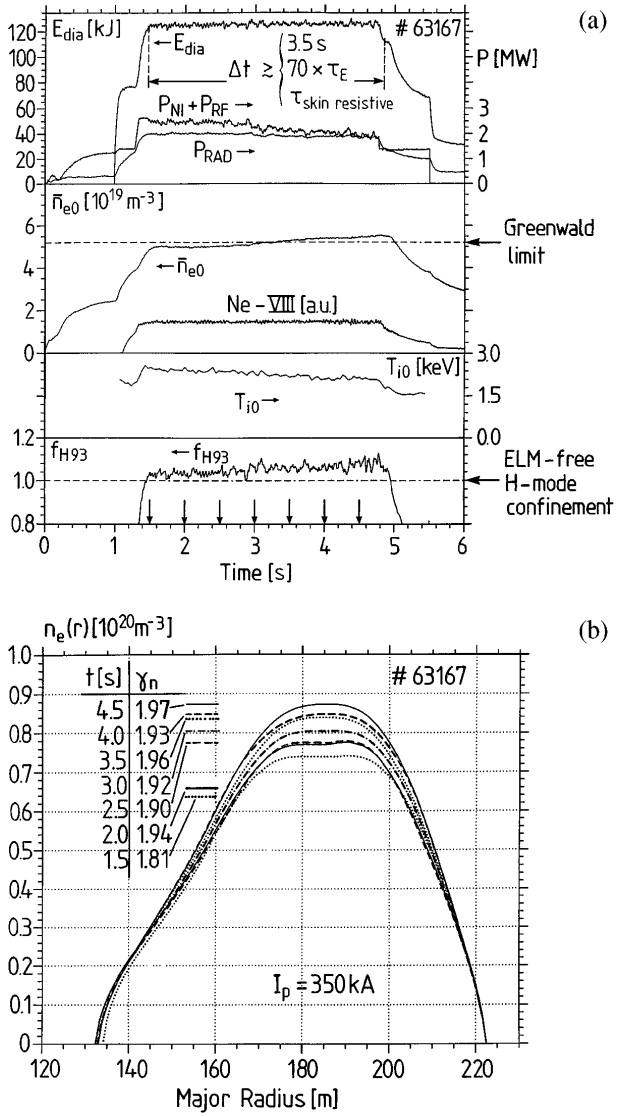

FIG. 1. (a) Typical example of a discharge obtained on TEXTOR-94 with feedback controlled energy content and edge neon impurity seeding. Shown are as a function of time, the signal of the diamagnetic energy $E_{\rm dia}$, the enhancement factor $f_{\rm H93}$ with respect to ITERH93-P, the central ion temperature T_{i0} from CXES of a CVI line, the line-averaged central density $\overline{n}_{e0}$, the total applied additional heating power $P_{\rm NI} + P_{\rm RF}$, the total radiated power $P_{\rm rad}$, and the intensity of the Ne VIII line. The dashed lines indicate the Greenwald density limit and ELM-free *H*-mode confinement. (b) Density profiles at the times indicated by the arrows in 1(a), where γ_n is the density profile peaking factor.

scaling ITERH93-P [9] for the divertor ELM-free *H* mode: It is larger than one for the whole duration of the neon seeding phase. This shows that we have a discharge with a confinement at least as good as ELM-free *H* mode. Note also the long duration of this phase, which is about 3.5 s or 70 confinement times (and also about equal to the resistive skin time) and is only limited by the flux swing capability of the OH transformer.

The gradual increase of the confinement as a function of time is linked to the slight rise in density. This is also reflected in the signal for the total applied additional heating power, which is steadily decreasing as a consequence of the feedback system. The relative decrease of $P_{\rm tot}$ is larger than the increase of $f_{\rm H93}$ according to the relation $P_{\rm tot}(f_{\rm H93})^3 \cong$ const as follows from the ITERH93-P scaling.

Note that, in the second half of the heating pulse, the density reaches values above the Greenwald upper density limit ($\overline{n}_{e0,\rm Greenwald} = I_p/\pi a^2$ using as units 10^{20} m^{-3}, MA, m) [10] which has a considerable empirical verification when gas puff fueling is employed. The density profiles shown in Fig. 1(b) are characterized by a peaking factor $\gamma_n = n_e(0)/\langle n_e(r)\rangle \cong 2$ with central density values attaining 10^{20} m^{-3}, in contrast to the flat profiles obtained in *H* mode. Improved confinement at these high densities is not due to fast particle contributions as follows from the comparison of the diamagnetic and equilibrium (MHD) plasma energies and from TRANSP simulations. The equipartition time is about equal to the energy confinement time $\tau_E \cong 50$ ms, and the discharges exhibit a slightly higher temperature for the ions than for the electrons.

Confinement properties.—A summary of the confinement data obtained is shown in Fig. 2, where the values of $f_{\rm H93}$ as a function of the central chord line-averaged density are plotted at a plasma current $I_p = 0.35$ MA. Several important features are visible in this figure: (i) the energy confinement is increasing with increasing density as already observed in the *Z* mode of ISX-B [11], (ii) the best confinement data are obtained at sufficiently high radiation levels ($\gamma > 60\%$), and (iii) high densities are reached, up to 1.2 times the Greenwald limit, where the plasma energy is nearly thermal. β_n and β_p values increase with density to about 1.8 and 1.3, respectively, at the highest densities

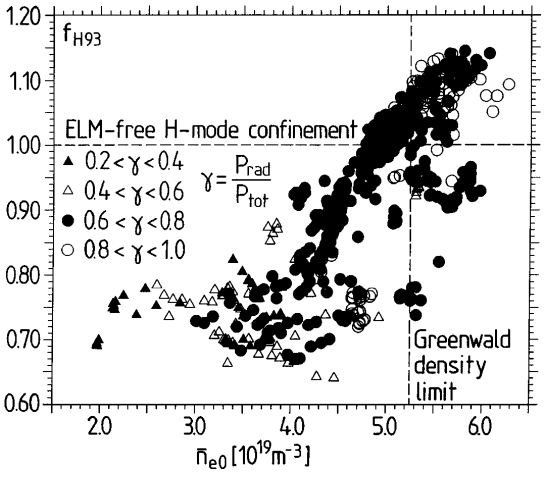

FIG. 2. Enhancement factor $f_{\rm H93}$ with respect to ITERH93-P versus line-averaged density at a plasma current $I_p = 350$ kA. The dashed lines indicate the Greenwald density limit and ELM-free *H*-mode confinement.

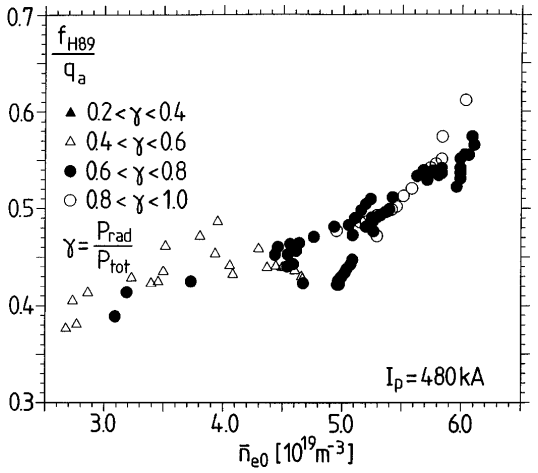

FIG. 3. Values for the figure of merit for ignition margin, f_{H89}/q_a, at a plasma current $I_p = 480$ kA.

reached. The marked increase of the enhancement factor f_{H93} with density is in contrast to the ITERH93-P scaling which shows a much weaker density dependence ($\propto \bar{n}_{e0}^{0.17}$) for the ELM-free H mode.

A large value of f_{H89}/q_a (with f_{H89} the enhancement factor with respect to the L-mode scaling ITERL89-P [12] and q_a the cylindrical safety factor at the plasma boundary) is important because the fusion triple product scales as the square of this parameter (the so-called figure of merit for ignition margin). As shown in Fig. 3, maximum values for f_{H89}/q_a are found at the highest densities reached and are around 0.6, the value required for ITER.

Radiation and impurities.—With an increasing radiation level, the radiating belt at the plasma boundary becomes poloidally more symmetric as shown in Fig. 4, indicating the dominance as a radiator of the seeded impurity neon over the intrinsic impurities C and O, which radiate more in the vicinity of the toroidal belt limiter ALT-II. The Li- and Be-like states of Ne, having a larger ionization time than the intrinsic impurities and thus being more uniformly distributed, account for most of the radiation (maximum values of 0.62 MW/m^3 in the radiation belt, which extends up to $T_e = 150$ eV). There is only a small contribution to the total radiated power from the central plasma, where the hydrogenlike, heliumlike, and fully ionized neon ions are located. The data displayed in Fig. 5 illustrate the stationarity of different impurity related plasma parameters (brilliance of D_α and impurity lines, neutron yield, and total radiated power) and of the enhancement factor f_{H93} during the additional heating phase. Small variations are due to an increase in the electron density, largely caused by limitations in the feedback system and could possibly be overcome by acting on the pumping capability of ALT-II and on the wall recycling. Note that the D_α signal does not show any sign of ELMs and the small oscillations seen are correlated with oscillations in the feedback system for the horizontal plasma position. We find that these plasmas with a radiating belt are thermally stable [13], quasistationary, and do not show MARFEs [3]. Furthermore, they are free of central impurity accumulation as seen from the constant ratio of the brilliance of atoms at the edge, representing the neutral impurity flux into the plasma, and of highly ionized stages in the bulk plasma (Ne and C; see Fig. 5) and from the neutron reactivity.

The most direct evidence of the absence of deleterious effects of the seeded impurity on the central plasma purity is the comparison of the neutron yield at different levels of neon seeding. The neutron yield, which in our case is

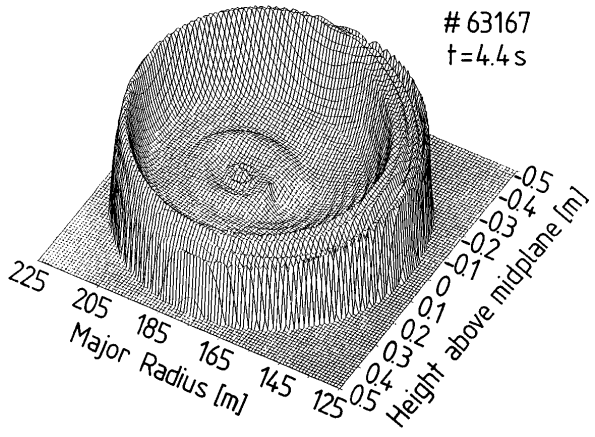

FIG. 4. Tomographic reconstruction of the radiation pattern in the discharge of Fig. 1 (from bolometry) at $t = 4.4$ s.

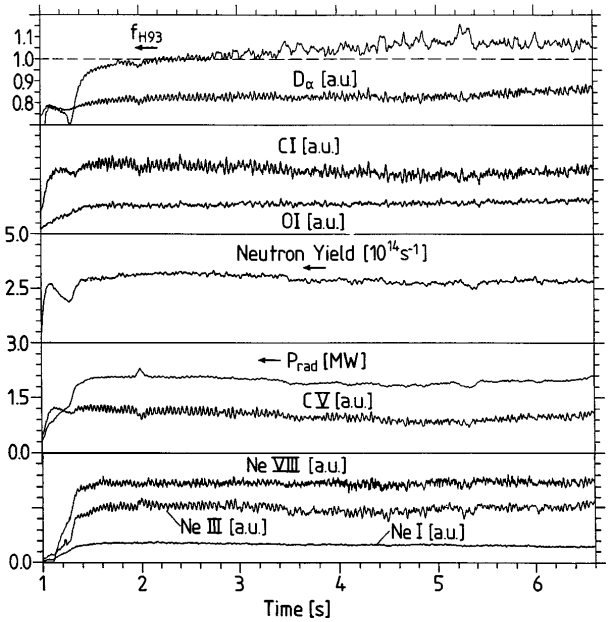

FIG. 5. Example of the quasistationarity of the impurity content of radiatively cooled discharges. Shown are as a function of time, the intensity of a line of Ne VIII, Ne III, Ne I, C V, C I, O I, and D_α, the radiated power P_{rad}, the neutron yield, and the enhancement factor f_{H93} for the energy confinement time versus ITERH93-P.

dominated by beam-target reactions, is mainly proportional to $n_{D0}/n_{e0}f(T_{e0})$ for a given injection energy and power, where n_{D0}/n_{e0} expresses the target fuel dilution. We find that for a given T_{e0} the neutron yield is always equal or higher with neon seeding [5,13]. A careful comparison of the neutron yield between discharges of the same series with and without neon seeding leads to roughly the same target fuel dilution in both cases. This means that the bulk neon concentration is compensated by a decrease of the intrinsic impurities. This can result from a reduced sputtering of wall material due to a lower edge temperature as explained in [14]. Note that although the dilution is the same, Z_{eff} will increase when the atomic number of the seeded impurity is larger than that of the intrinsic impurities.

An estimate of the neon concentration in the plasma volume follows also from a detailed particle balance for the seeded neon. Altogether this leads to an estimated average concentration of about 1.5% Ne for discharge conditions as shown in Figs. 1 and 5. Such a neon concentration agrees with an estimation of the mean Z_{eff} value obtained from visible bremsstrahlung which increases from 2.2 in a reference discharge (in the same conditions as for the shot of Fig. 1, but without neon injection and $\overline{n}_{e0} = 4.2 \times 10^{19}$ m^{-3}) to the value of 2.6 for the discharge shown in Fig. 1. The slight increase of Z_{eff} can be understood by the decrease of the intrinsic impurity content as explained above.

Whether these results can be applied to a burning fusion plasma in a machine with the size of, e.g., ITER is still uncertain due to the lack of knowledge concerning the mechanisms of impurity transport—a common problem to all types of high confinement discharge scenarios (on divertor or limiter machines). The maximum amount of seeded impurities in a burning plasma is further constrained by the level of He ash which depends on the balance between production and exhaust. The latter could be the most critical part, since already the value of $\tau_p^*/\tau_E = 10$ as considered for ITER [15] leaves a rather small margin for impurities other than He. In this respect, gaining a better knowledge of impurity transport in reactor grade plasmas is of utmost importance and requires further study. Besides absolute values, we would like to note that the best confinement of these plasmas is obtained at the highest electron densities achieved, thus for conditions where several aspects are optimal: high value for the fusion triple product, best pumping capabilities, and minimum seeded impurity concentration for a given P_{rad}, since P_{rad} increases strongly with n_e for a given impurity concentration [16].

In conclusion, a new operational regime possibly suitable for use in a future fusion reactor has been identified on TEXTOR-94. It combines the following attractive features: On top of high confinement, high density, high plasma β, and the promising heat removal capabilities by radiation it is characterized by (i) absence of ELMs, absence of a power threshold; (ii) presence of peaked density profiles facilitating ignition; (iii) a strong increase of the confinement with density which minimizes the amount of impurities needed for a given radiation fraction γ and leads to a favorable pumping efficiency of the pumped limiter; and (iv) a concentration for the seeded impurity sufficiently low to avoid detrimental effects on the fusion reactivity. Note that these discharges are obtained in a pumped limiter tokamak thereby avoiding the need of a (radiating) divertor.

As the influence of the machine size on these results is not known, extrapolation to larger machines has to be assessed experimentally anyway for what concerns energy and particle (D, T, and impurities) transport.

*Also at NFSR, Belgium.

[1] J. Ongena *et al.,* Nucl. Fusion **33**, 283–300 (1993).
[2] R. Zarnstorff *et al.,* in *Plasma Physics and Controlled Nuclear Fusion Research, Würzburg 1992* (International Atomic Energy Agency, Vienna, 1993), Vol. I, p. 111.
[3] U. Samm *et al.,* Plasma Phys. Controlled Fusion **35**, B167 (1993).
[4] J. Winter *et al.,* Phys. Rev. Lett. **71**, 1549 (1993).
[5] A. M. Messiaen *et al.,* Nucl. Fusion **34**, 825 (1994).
[6] O. Gruber *et al.,* Phys. Rev. Lett. **74**, 4217 (1995).
[7] K. H. Dippel *et al.,* J. Nucl. Mater. **145–147**, 3 (1989).
[8] J. Ongena *et al.,* Plasma Phys. Controlled Fusion **38**, 279 (1996).
[9] D. P. Schissel *et al.,* in *Proceedings of the 20th European Conference on Controlled Fusion and Plasma Physics, Lisbon* (European Physical Society, Geneva, 1993), Vol. 17C, Pt. I, p. 103; K. Thomsen *et al.,* Nucl. Fusion **34**, 131 (1994).
[10] M. Greenwald *et al.,* Nucl. Fusion **28**, 2199 (1988).
[11] E. A. Lazarus *et al.,* Nucl. Fusion **25**, 135 (1985).
[12] P. N. Yushmanov *et al.,* Nucl. Fusion **30**, 1999 (1990).
[13] A. M. Messiaen *et al.,* Nucl. Fusion **36**, 39 (1996).
[14] G. Telesca *et al.,* in *Proceedings of the 21st European Conference on Controlled Fusion and Plasma Physics, Montpellier* (European Physical Society, Geneva, 1994), Vol. 18B, Pt. II, p. 806; Nucl. Fusion **36**, 347 (1996).
[15] G. Janeschitz and ITER team, Plasma Phys. Controlled Fusion **37**, Suppl. 11A, A19 (1995).
[16] M. Z. Tokaŕ, Nucl. Fusion **34**, 853 (1994).